Control of light transmission through opaque scattering media in space and time

Jochen Aulbach,[1,2,*] Bergin Gjonaj,[1] Patrick M. Johnson,[1] Allard P. Mosk,[3] and Ad Lagendijk[1]

[1]*FOM Institute for Atomic and Molecular Physics AMOLF, Science Park 113, 1098 XG Amsterdam, The Netherlands*

[2]*Institut Langevin, ESPCI ParisTech, CNRS, 10 rue Vauquelin, 75231 Paris Cedex 05, France*

[3]*Complex Photonic Systems, MESA+ Institute for Nanotechnology and Department of Science and Technology, University of Twente, Post Office Box 217, NL-7500 AE Enschede, The Netherlands*

Abstract

We report the first experimental demonstration of combined spatial and temporal control of light trajectories through opaque media. This control is achieved by solely manipulating spatial degrees of freedom of the incident wavefront. As an application, we demonstrate that the present approach is capable to form bandwidth-limited ultrashort pulses from the otherwise randomly transmitted light with a controllable interaction time of the pulses with the medium. Our approach provides a new tool for fundamental studies of light propagation in complex media and has potential for applications for coherent control, sensing and imaging in nano- and biophotonics.

Concentrating light in time and space is critical for many applications of laser light. Broad-band mode-locked lasers provide the required ultrashort light pulses for multiphoton imaging [1, 2], nanosurgery [3], microstructuring [4], ultrafast spectroscopy [5, 6] and coherent control of molecular dynamics or of nanooptical fields [7–9]. Multiple random scattering in complex media severely limits the performance of these methods, but often is an unavoidable nuisance in many systems of interest, such as biological tissue or nanophotonic structures [10]. Spatially, random scattering strongly distorts a propagating wave front, creating the well-known speckle interference pattern [11]. In the time domain, ultrashort pulses are strongly distorted and widely stretched due to the broad path length distribution in multiple scattering media [12]. These temporal and spatial distortions are not separable [13].

There is a strong interest in improving applications of ultrashort laser pulses in complex scattering media. Phase conjugation has been applied to spatially focus light from a short-pulse laser source through a thin scattering layer [14]. Similarly, phase conjugation is applied to correct distortions of the ballistic wave front to improve the resolution of two photon microscopy [15]. Coherent control of two-photon excitation through scattering biological tissue has been demonstrated [16]. Those experiments share the common limitation that the control is limited only to those photons that take the shortest paths through the disordered media and arrive a the target volume without being multiply scattered.

Recently it was demonstrated that random scattering can actually be beneficial rather than detrimental for the performance of optical systems. Applying a shaped wave front of monochromatic light to a strongly scattering medium, Vellekoop et al. achieved spatial control over the scattered light [17]. In fact, the insertion of an opaque sample after a lens has allowed focusing beyond the diffraction limit of the lens [18]. These findings have opened new possibilities for imaging in optically thick biological matter [19] and allow trapping particles through turbid media [20]. Related techniques which allow coherent focusing in scattering media are known from ultrasound [21] and microwaves [22]. The frequency of those types of waves is low enough that electronic transducers can be used to time reverse waves, which redirects the waves towards their source. This technique has successfully helped to improve imaging resolution [23] and communication bandwidth [24].

In this Letter we report the first experimental demonstration of combined spatial and temporal control of light trajectories through opaque media via spatial wavefront shaping.

We apply our method to create an ultrashort pulse from the light transmitted through a strongly scattering medium. We can control the amount of time the optimized pulse stays in the sample and thereby select the path length of the light through the medium. The efficiency of our method is independent of the time delay, allowing for ultrashort pulses to be formed even from very long paths in the sample.

The experimental realization can be summarized as follows (Figure 1). An short-pulse

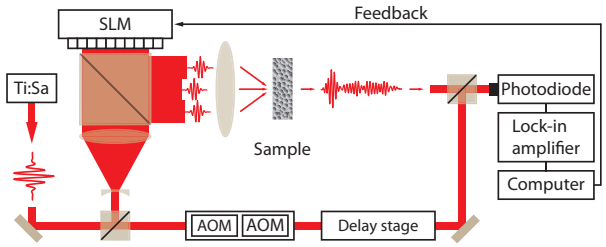

FIG. 1: Experimental setup. A beam from a mode-locked Titanium:Sapphire (Ti:Sa) laser is coupled into a heterodyne Mach-Zehnder interferometer. In the signal branch the beam reflects off a spatial light modulator (SLM) and is subsequently focused onto the sample. The light in the reference branch is frequency shifted by 40 kHz by two acousto-optical modulators (AOM) and then passes through a motorized delay line. The signal from the detector is filtered by a lock-in amplifier (LIA) and recorded by the Computer.

light source illuminates a phase-only spatial light modulator (SLM), which can alter the phase of the light reflected from its surface. The SLM pixels are grouped into N independent segments each of which induces a controllable phase shift $\Delta\Phi_i$, which can be considered constant over the bandwidth of the laser. The scattering sample is placed in the Fourier plane of the SLM. Both SLM and sample are embedded in the signal arm of a heterodyne Mach-Zehnder-type interferometer [25]. The heterodyne signal exactly corresponds to the cross-correlation of the of the forward scattered pulse with the reference pulse, which is delayed by a variable time delay τ. The reference pulse is close to Fourier-limited, so that amplitude and phase of the transmitted pulse will not change significantly over the duration of the reference pulse. The heterodyne signal is then effectively an instantaneous measurement of the transmitted electric field. This signal serves as a feedback for an optimization algorithm, which programs the SLM. The time delay of the reference pulse is adjusted by an automated delay stage allowing optimization at a desired point in time τ_{opt}. An extended description of the setup including technical details has been included in the supplementary

material.

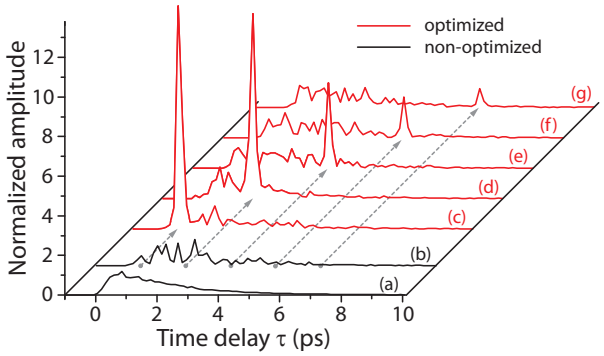

FIG. 2: Optimized and random speckle pulses. (a) Amplitude of heterodyne signal of a non-optimized pulse as a function of time delay, averaged over 50 random speckle pulses. (b) Typical single random speckle pulse. (c)-(g) Amplitudes of single pulses after optimization at different time delays which are indicated by the dashed arrows. The optimization has been performed by dividing the SLM into 300 segments. The optimization generates strong, short pulses from diffuse light. The zero delay position is at the maximum amplitude with no sample. The plotted curves have been normalized to the maximum of the average non-optimized heterodyne signal (factor 1.53 mV^{-1}).

The principle of the experiment can be described as follows. Light reflected from a single segment on the SLM is transmitted through the sample, giving rise to the field $E_i(t)$ at the detector. Its phase can be modified by a time-independent phase shift $\Delta\Phi_i$ via the SLM. The total field scattered into the detector $E_{out}(t)$ is therefore given by the sum over all segments

$$E_{\mathrm{out}}(t) = \sum_{i=1}^{N} E_i(t) e^{i\Delta\Phi_i}. \tag{1}$$

Multiple scattering allows us to assume that the contributions $E_i(t)$ from the different segments at every single point in time t are uncorrelated random variables with Rayleigh distributed amplitudes $|E_i(t)|$ and uniformly distributed phases $\Phi_i(t)$ [26]. For the non-optimized case, the resulting field $E_{\mathrm{out}}(t)$ can be viewed as the result of a random walk in the complex field plane. After the optimization, all contributions are in phase, adding up

constructively. The average amplitude enhancement is given by [17]

$$\begin{aligned}\langle\alpha\rangle &= \frac{\langle|E_{\rm opt}|\rangle_{\rm rms}}{\langle|E_{\rm rnd}|\rangle_{\rm rms}} \\ &= (\frac{\pi}{4}(N-1)+1)^{1/2} \approx (\frac{\pi}{4}N)^{1/2}. \end{aligned} \quad (2)$$

The average intensity enhancement η can be obtained by $\eta = \alpha^2$.

The non-optimized data was obtained by setting random phase values to the SLM segments. The optimization algorithm adjusts the phase shifts $\Delta\Phi_i$ such that the amplitude of the heterodyne signal is maximized. We performed the optimization at 20 equidistant time delays $\tau_{\rm opt}$ between -1.05 ps to +13.6 ps. For each $\tau_{\rm opt}$, the optimization was performed four times, with N = 12, 48, 192 and 300 segments, respectively, each time starting from a new random phase pattern.

Our main result is displayed in Figure 2, showing the amplitudes of both the non-optimized (black lines) and the optimized (red lines) pulses for different time delays $\tau_{\rm opt}$ and N = 300 segments on the SLM. The optimized amplitudes show sharp, distinct peaks with dramatically increased amplitudes at the desired time delay. We can control the amount of time the optimized pulses stay in the sample by the time delay $\tau_{\rm opt}$, and by that we control the path length of the pulses through the sample. Note that the heterodyne signal is proportional to the field amplitude, the intensities exhibit even more pronounced optimized peaks.

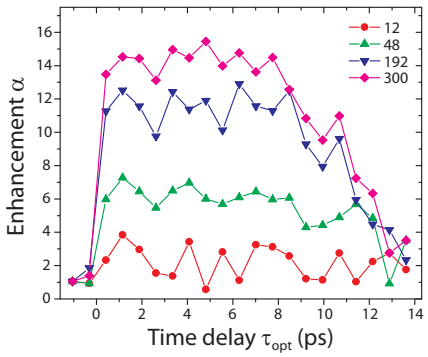

FIG. 3: Enhancement α versus selected time delay $\tau_{\rm opt}$ for different number of segments N on the spatial light modulator.

The enhancement α versus time delay $\tau_{\rm opt}$ is shown in Figure 3. Its magnitude, depending on the number of segments on the SLM, is constant from zero to several picoseconds time

delay. This result shows that our method works for short light paths as well as for light paths more than ten times longer than the sample thickness.

For long time delays a continuous decrease of α is observed, which is related to the noise level of the experiment. We include a quantitative analysis of this effect in the supplementary material.

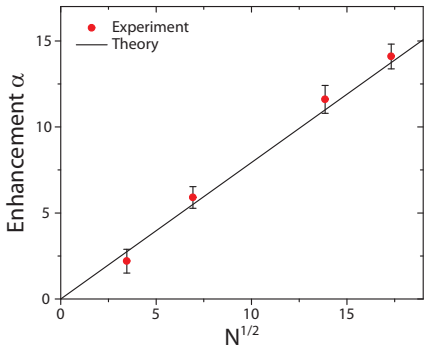

FIG. 4: Average amplitude enhancement α (red dots) as a function of the square root of the number of segments N. The solid line is given by the expected $\alpha = 0.90\,(\frac{\pi}{4}N)^{1/2}$, without any free parameter.

Figure 4 shows the average enhancement in the constant regime in Figure 3 versus N together with the enhancement expected from theory (Eq.2), $\langle\alpha\rangle = \sigma(\frac{\pi}{4}N)^{1/2}$. The prefactor $\sigma = 0.90$ corrects for the non-uniform illumination of the SLM surface with a truncated Gaussian beam, which effectively leads to a reduction of the number of used segments (see supplementary material). Our model matches the data well with no adjustable parameters.

We have investigated the duration of optimized pulses in detail. Figure 5 shows the heterodyne signal of three typical optimized pulses in a detailed scan of the time delay around the respectively chosen optimization time τ_{opt}. The average width of the optimized peaks (full width at half maximum) $\Delta\tau_{\mathrm{opt}} = 190 \pm 7\,\mathrm{fs}$, shows no dependence on time delay range between zero and 10 ps. The heterodyne signal is given by the amplitude of the optimized pulses, convoluted with the bandwidth-limited reference pulses. By deconvolution we calculated the field amplitude of the optimized pulses and determined their (intensity) pulse duration $\Delta\mathrm{t}_{\mathrm{opt}}$. The optimized pulses have a duration $\Delta\mathrm{t}_{\mathrm{opt}} = 115$ fs. For comparison, the input pulses have a transform-limited duration of $\Delta\mathrm{t}_{\mathrm{in}} = 64$ fs. This raises the question whether the lengthening of the transmitted pulse is caused by spectral narrowing or by remaining fluctuations of the spectral phase. Numerical simulations, which are appended in

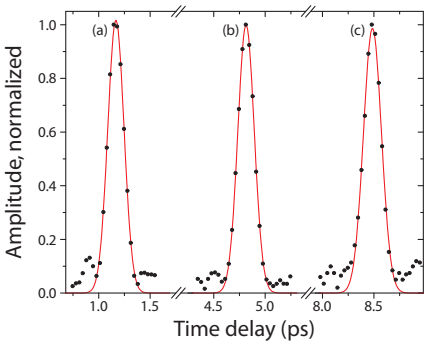

FIG. 5: Detailed cross-correlation scans around the optimized pulses at the time delays $\tau_{\mathrm{opt}} = 1.1$ ps (a), 4.8 ps (b) and 8.5 ps (c), together with a Gaussian fit (red lines). The amplitudes have been normalized to the maximum of the respective peak. The width (FWHM) of the peaks are $\Delta\tau_{\mathrm{opt}} = 186$ fs (a), 188 fs (b) and 206 fs (c). These values are typical in the range of time delays between zero and 10 ps, with an average width $\Delta\tau_{\mathrm{opt}} = (190 \pm 7)$fs.

the supplementary material, show that the answer is dependent on the number of segments N. For a low number of segments, the spectrum of the optimized pulse is random with a very short frequency correlation, but overall retains the shape and the width of the Gaussian input spectrum. The optimized spectral phase is not flat so that the pulses do not reach the bandwidth limit. For an increasing number of segments, the duration of the optimized pulse converges to its Fourier-limit. The spectrum has a smooth Gaussian shape, but a bandwidth narrower than the input spectrum. The method is capable of creating bandwidth-limited pulses, but since it is based on linear interferometry, the adaption to other pulse shapes is equally possible.

The time-integrated intensity (energy) of the pulse with the highest peak depicted in Figure 2 is 13.5 times higher than the energy of the average non-optimized pulse. In addition to the temporal optimization, overall more light is transmitted into the detected channel, demonstrating that the scattered light is controlled spatially and temporally. Our method exploits the mixing of spatial and temporal degrees of freedom by the random medium [13], to control the transmitted light in two spatial and one temporal dimension by only controlling spatial degrees of freedom on the two-dimensional SLM. On the one hand, the conversion of spatial degrees of freedom into temporal ones comes to the price of a speckle background, which on the other hand is easily outweighed by the enormous number of degrees of freedom provided by state-of-the-art SLMs. The large number of controllable spatial

degrees of freedom is a great advantage over frequency domain pulse shaping techniques. Spatiotemporal control of the light field allows a far more generalized application of present coherent control schemes and marks a further step towards optical time reversal.

In the experimental realization presented here, we optimized the pulse front using linear interferometry as feedback signal. The optimization of a non-linear response, like second-harmonic generation, will also lead to a comparably optimized pulse [27]. Using a nanoparticle with a non-linear emission response [14] then enables the focusing of ultrashort pulses inside complex scattering media. We envision that our method can improve approaches for selective cell destruction in tissue [28]. In view of its potential for sharp focussing, it has potential for nanofabrication, nanosurgery and other micromanipulation techniques.

Up to now we have not discussed the spatial extent of the optimized pulse. We use an aperture to select a single speckle spot in the Fourier plane of the sample for optimization, which corresponds to light transmitted into the forward direction. We know that transmitted fields in adjacent speckle spots are uncorrelated [29], from which we can conclude that the optimization is indeed limited to the selected area. An important future direction would be to investigate the spatial extent of the optimized pulse as a function of delay time. A combination with spatial scanning allows the measurement of the transmission matrix of the medium [30] in one temporal and two spatial dimensions. For Anderson-localizing samples [31], the size of the optimized speckle should be strongly time-dependent [32].

In conclusion, we have experimentally demonstrated that spatial wave front shaping of a pulse front incident on a strongly scattering sample gives spatial and temporal control over the scattered light. Our approach provides a new tool for fundamental studies of light propagation and has potential for applications in sensing, nano- and biophotonics.

We thank Timmo van der Beek for the sample fabrication, Kobus Kuipers for providing the AOMs and Huib Bakker for helpful comments on the manuscript. This work is part of the Industrial Partnership Programme (IPP) Innovatie Physics for Oil and Gas (iPOG) of the Stichting voor Fundamenteel Onderzoek der Materie (FOM), which is supported financially by Nederlandse Organisatie voor Wetenschappelijk Onderzoek (NWO). The IPP MFCL is co-financed by Stichting Shell Research.

---

* Electronic address: j.aulbach@amolf.nl

[1] S. W. Hell and J. Wichmann, Opt. Lett. **19**, 780 (1994).

[2] W. R. Zipfel, R. M. Williams, and W. W. Webb, Nat. Biotechnol. **21**, 1369 (2003).

[3] A. Vogel *et al.*, Appl. Phys. B **81**, 1015 (2005).

[4] E. N. Glezer *et al.*, Opt. Lett. **21**, 2023 (1996).

[5] A. H. Zewail, J. Phys. Chem. A **104**, 5660 (2000).

[6] J. Shah, *Ultrafast spectroscopy of semiconductors and semiconductor nanostructures* (Springer, 1999).

[7] H. Rabitz *et al.*, Science **288**, 824 (2000).

[8] J. Herek *et al.*, Nature **417**, 533 (2002).

[9] M. Aeschlimann *et al.*, Nature **446**, 301 (2007).

[10] A. F. Koenderink and W. L. Vos, Phys. Rev. Lett. **91**, 213902 (2003).

[11] J. Dainty, *Laser Speckle and Related Phenomena* (Springer, 1984).

[12] A. Z. Genack and J. M. Drake, Europhys. Lett. **11**, 331 (1990).

[13] F. Lemoult *et al.*, Phys. Rev. Lett. **103**, 173902 (2009).

[14] C. Hsieh, *et al.*, Opt. Express **18**, 12283 (2010).

[15] M. Rueckel, J. A. Mack-Bucher, and W. Denk, Proc. Natl. Acad. Sci. USA **103**, 17137 (2006).

[16] J. M. D. Cruz *et al.*, Proc. Natl. Acad. Sci. USA **101**, 16996 (2004).

[17] I. M. Vellekoop and A. P. Mosk, Opt. Lett. **32**, 2309 (2007).

[18] I. M. Vellekoop, A. Lagendijk, and A. P. Mosk, Nature Photon. **4**, 320 (2010).

[19] E. J. McDowell *et al.*, J. Biomed. Opt. **15**, 025004 (2010).

[20] T. Cizmar, M. Mazilu, and K. Dholakia, Nature Photon. **4**, 388 (2010).

[21] A. Derode, P. Roux, and M. Fink, Phys. Rev. Lett. **75**, 4206 (1995).

[22] G. Lerosey *et al.*, Science **315**, 1120 (2007).

[23] M. Fink and M. Tanter, Phys. Today **63**, 28 (2010).

[24] S. H. Simon *et al.*, Phys. Today **54**, 38 (2001).

[25] M. Sandtke *et al.*, Rev. Sci. Instrum. **79**, 013704 (2008).

[26] B. A. van Tiggelen *et al.*, Phys. Rev. E **59**, 7166 (1999).

[27] D. Yelin, D. Meshulach, and Y. Silberberg, Opt. Lett. **22**, 1793 (1997).

[28] C. Loo *et al.*, Nano Lett. **5**, 709 (2005).

[29] P. Sebbah, *Waves and Imaging Through Complex Media* (Springer, 2001).

[30] S. M. Popoff *et al.*, Phys. Rev. Lett. **104**, 100601 (2010).

[31] P. W. Anderson, Phys. Rev. **109**, 1492 (1958).

[32] S. E. Skipetrov and B. A. van Tiggelen, Phys. Rev. Lett. **96**, 043902 (2006).